

Effect of Different Conductive Additives on the Electrochemical Properties of Mesoporous MnO₂ Nanotubes

Xiao Wang, Xiaoli Liu, Ke Chen*

College of Materials Science and Engineering, Chongqing University, Chongqing 400044, PR China

*E-mail: chenke1_cqu@163.com;

Received: 30 April 2016 / Accepted: 5 June 2016 / Published: 7 July 2016

MnO₂ as an environmental benignity material has been of great interest for supercapacitors due to its unique properties leading to improved performances. Herein we describe the effects of different conductive agent to improve the electrochemical properties of MnO₂ nanotubes. Three typical conductive additives: carbon black, carbon nanotubes, and graphene are chosen to mix with MnO₂ nanotubes in the working electrodes. The specific conductivities of MnO₂@carbon black particles electrode, MnO₂@carbon nanotubes electrode, and MnO₂@graphene electrode at the current density 1 A g⁻¹ are 244.8 F g⁻¹, 190.2 F g⁻¹, and 114.1 F g⁻¹ respectively. Furthermore, MnO₂@carbon nanotubes electrode possesses an electrochemical capacitance as high as 297.5 F g⁻¹ at the current density 0.5 A g⁻¹, which can be put down to these soft thin nanotubes can be intertwined with each other to form a powerful network to provide conduction. In principle, the high specific capacitance and stable structure of the MnO₂@carbon nanotubes electrode ensures its potential for the applications in supercapacitors and other microelectronics.

Keywords: graphene; carbon blacks; carbon nanotubes; manganese dioxide nanotubes; supercapacitors

1. INTRODUCTION

With the rapid development of the technologies, energy grows to a crisis to the world. The technological thereupon advances such as full cells, supercapacitors for high-performance energy storage devices. It is well-documented that the high power densities, fast charge-discharge rates, and excellent cyclic stabilities can be owned by using supercapacitors [1-5]. The mechanism of supercapacitors can be divided into two different types. The electrical double-layer is from charge separation to obtain electrostatic storage, while pseudocapacitors based on the reversible Faradic reactions [6-8].

Transition metal oxides provide opportunities to design electrodes for supercapacitors with high performance. As for transition metal oxide, such as RuO_2 , it has high theoretical capacity; however, its toxic feature and high cost limit its utility [9-10]. MnO_2 as an environmental benignity material has been of great interest for supercapacitors due to its unique properties leading to improved performances. However, its poor electrical conductivity is the issue to use in practical supercapacitors [11-14]. A nanoscale approach to electrodes for supercapacitors has been more popular in recent years, various morphologies have been reported before, such as nanosheet arrays, nanoparticles, core/shell nanostructures, tubular arrays and so on [4,12,15-17]. Recent researches have proven that hollow structures can improve the electrochemical properties for supercapacitors compared to solid nanostructures [18]. The use of MnO_2 nanotubes as electrode in our experiment has many advantages: (i) improved electrical conductivity due to the high porosity (ii) low internal resistance due to hollow 1D conductive paths, (iii) large active area and ability to withstand cyclic changes in volume [19-20].

In order to explore the improvement of different conductive agent for MnO_2 electrodes, some research also have done by using different conductive additives to improve the electrical conductivities, especially by adding carbon nanostructures and graphene to modify the capacitor properties and cycling stabilities. In addition, carbon nanostructures and graphene are both allotropes of carbon, and the compositions and morphologies of the conductive additives define the electrode in specific capacitance, discharge rate, and cycle life as well [10, 21-25]. Porous carbon black (CB) particles as the 0D conductive agent are widely used electrode materials due to their large surface area, moderate cost, and relatively good electrical properties in specific capacitance, discharge rate, and cycling stability [25-26]. Carbon nanotubes possess a cylindrical hollow 1D nanostructure which was made up with carbon sheets in the size of several atoms, and ultimately determines its properties of rapid charge-discharge rate [27-28]. Meanwhile, graphene has a theoretical specific surface area of $2630 \text{ m}^2 \text{ g}^{-1}$ due to its 2D honeycomb lattice which arranged into a planar monolayer of carbon atoms, and has a very high intrinsic electrical conductivity and chemical stability [29-30]. However, a typical comparative research had not been reported.

Herein, we firstly report that the different conductive additives for MnO_2 nanotubes, and their applications as electrodes for supercapacitor. MnO_2 nanotubes were synthesized by etching from CuO@MnO_2 composites, what's more, the reaction liquid after etching even provide Cu^{2+} to obtain other Cu and Cu oxide nanostructures for supercapacitors [31-32]. Carbon black particles, graphene, and carbon nanotubes were introduced to the unique hollow 1D nanostructure is expected to deliver exceptional electrochemical performance. The results indicate that the conductive additives indeed influence the performance of the supercapacitor and the graphene represent the best in terms of energy capacity and stability.

2. EXPERIMENTAL

2.1 Preparation of MnO_2 nanotubes

MnO_2 nanotubes were prepared by etching method from the CuO/MnO_2 core-shell architecture [33]. Briefly, CuO/MnO_2 core-shell architecture was corroded by 1 M H_2SO_4 and the resulting MnO_2

nanotubes were refined and purified via successive centrifugation in water and alcohol, then dried under 60 °C in air [30].

2.2 Homogeneous mixture of MnO₂ nanotubes and conductive additives for electrodes

The mixture of MnO₂ nanotubes and conductive additives is simple but effective. First, a certain amount of MnO₂ nanotubes and conductive additives were taken in the beaker, and marked A, B, C respectively on the beaker which added carbon black, carbon nanotubes, graphene. Then, suitable amount of alcohol were introduced to the beaker for ultrasonic process. And followed drying, the mixing is finished, and the homogeneous mixture is prepared with the proportion 7:2, what's more, the polyvinylidene fluoride (PVDF) in N-methyl-2-pyrrolidone (NMP) was introduced in the homogeneous mixture with the proportion 9:1 for preparing working electrodes.

2.3. Characterization and Electrochemical measurements

Morphologies were taken on the focused ion beam (Zeiss Auriga FIB/SEM). The chemical compositions were measured by powder X-ray diffraction (XRD, D/max 2500, Cu, K). To study the response of MnO₂ nanotubes with different conductive additives, a three-electrode system including a working electrode (as-prepared products), a platinum electrode and a reference (saturated calomel) electrode was applied. All of the electrochemical testing including cyclic voltammetry (CV), Galvanostatic charge-discharge (GCD) and electrochemical impedance spectroscopy (EIS), were using an electrochemical workstation (CHI 660E) in the 1 M Na₂SO₄ aqueous solution. CV techniques were carried out on the potential range from -0.2 V to 0.8V with rate 5-100 mV s⁻¹, GCD measurements were performed by using current densities range between 0.5 and 10 A g⁻¹ in the same potential range. And EIS were calculated with the frequency range 10 mHz -100 kHz.

3. RESULTS AND DISCUSSION

3.1. Structure and morphology

The transformation of the nanostructure to form MnO₂ nanotubes, as shown in Fig.1, involves two major steps: (i) Cu nanowires (Nws) acted as the template, and the MnO₂ nanosheets grow on the template by hydrothermal and (ii) the Cu Nws were etching by H₂SO₄(aq) to obtain the MnO₂ nanotubes. We can see from Fig.1a and b that the size of Cu Nws is about 100 nm, and the wires have soft texture. Morphology of the composite of MnO₂ nanosheets decorated on Cu Nws is shown in Fig.1c and d, suggesting that the hydrothermal can roughen the smooth texture of the nanostructure. The sample increased its width from 100 nm to 800 nm due to Cu Nws has surfaces covered by nanosheets. However, the length get shorten correspondingly, which may due to the Cu Nws were corroded partly in the process of hydrothermal synthesis and led to the fracture. Fig.1e and f is the SEM of MnO₂ nanotubes, which revealed that the acid treatment caused slightly changes on the

structure of the composite, the length get shorten and the width get widen further. But the sample preserved its relatively rough surface morphology and one can realize textural porosity on the tube surfaces. However, completeness of etching needs further exploration.

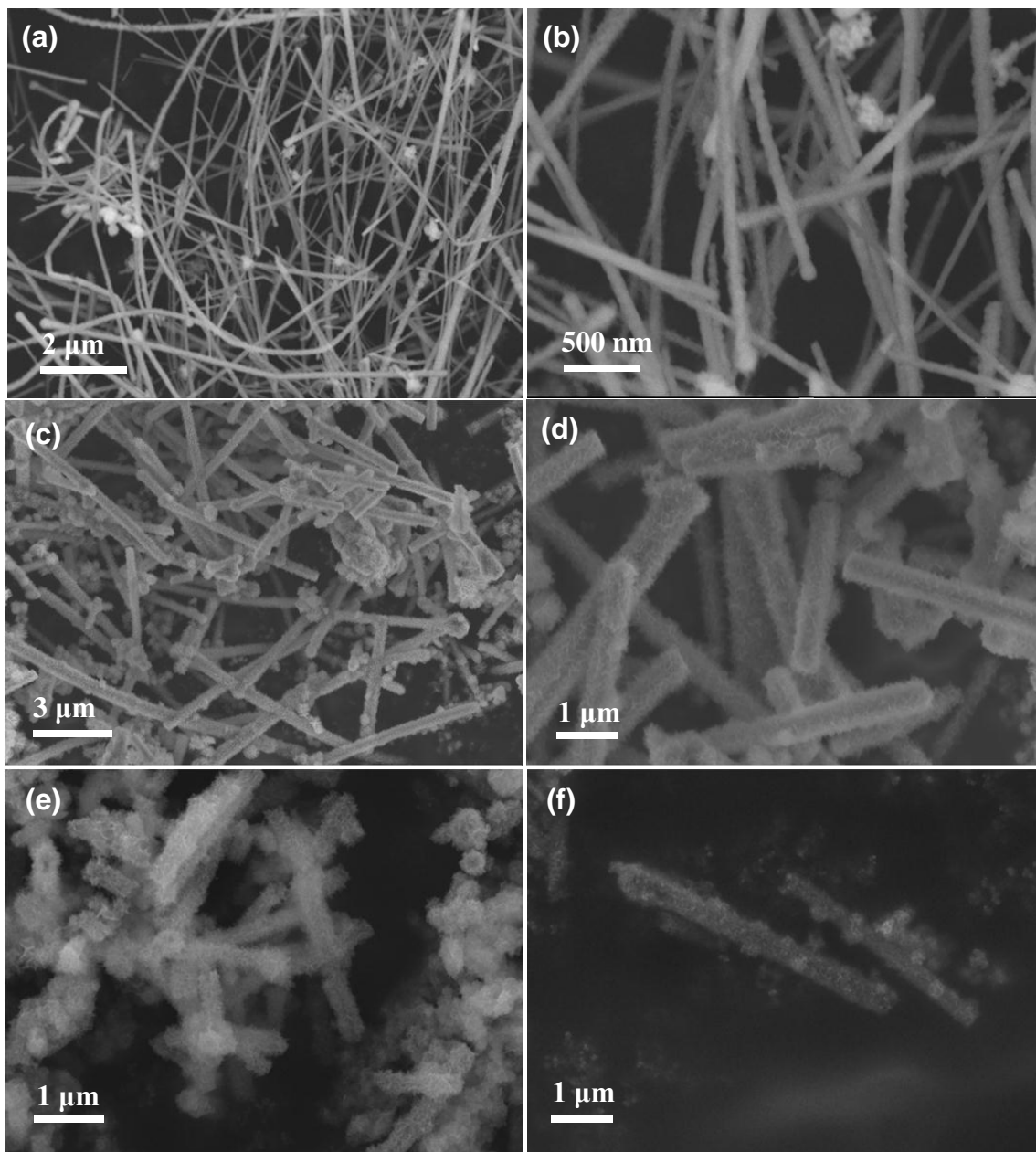


Figure 1. Typical SEM images of the Cu nanowires (a-b), CuO@MnO₂ nanostructure (c-d) and the MnO₂ NTs samples (e-f) at different magnifications.

X-ray diffraction (XRD) was conducted to firmly determinate the fineness of MnO₂ nanotubes. As show in the Fig.2a, the diffraction peaks at 12.7, 18.1, 25.6, 28.7, 37.6, 42.0, 49.9, 59.5, 65.5, 72.5, and 77.5° can be assigned to MnO₂ (JCPDS no.72-1982), which correspond to (110), (200), (220), (310), (121), (301), (411), (260), (002), (631) and (402) reflections, respectively. No other peaks were observed in MnO₂ nanotubes. This data indicate that the successful synthesis of the MnO₂ nanotubes

via our etching process. Fig.2b-d shows the SEM image of MnO₂ electrode with carbon black, carbon nanotubes, graphene respectively, and the corresponding SEM images of the conductive additives were shown in the inner plot. The SEM image in Fig. 2b offers the information on the mixture of MnO₂@carbon black electrode. The MnO₂ nanotubes provide the base material for carbon black to adjoin, and carbon black particles were gathered between the spaces of MnO₂ nanotubes. As all we knows that carbon black is the most common conductive additive used in electrochemical field due to its high capacitance, however, its property of easy to aggregation and point-to-point method in contact with activity materials may limit its efficiency. Fig. 2c depicts the SEM image of MnO₂ nanotubes with carbon nanotubes, which indicates that the carbon nanotubes have more flexible structure than MnO₂ nanotubes and and twine around the MnO₂ nanotubes to form a powerful pathway for charge transfer. The microstructures of carbon nanotubes are cylindrical and decorate with multiaperture structure as reported by and the unique structure benefit for the charge storage by the electric double-layer principle [27]. The good entangled network also contributes to the mechanical properties of the electrode. From Fig.2d, we can see that MnO₂ nanotubes were interspersed with plate structure of graphene, however, according to the real data of our work, the MnO₂ nanotubes show the uniformly width about 800 nm which is relatively large compared with graphene nanosheets, and the sheets between the MnO₂ nanotubes could not build an effective conductive network.

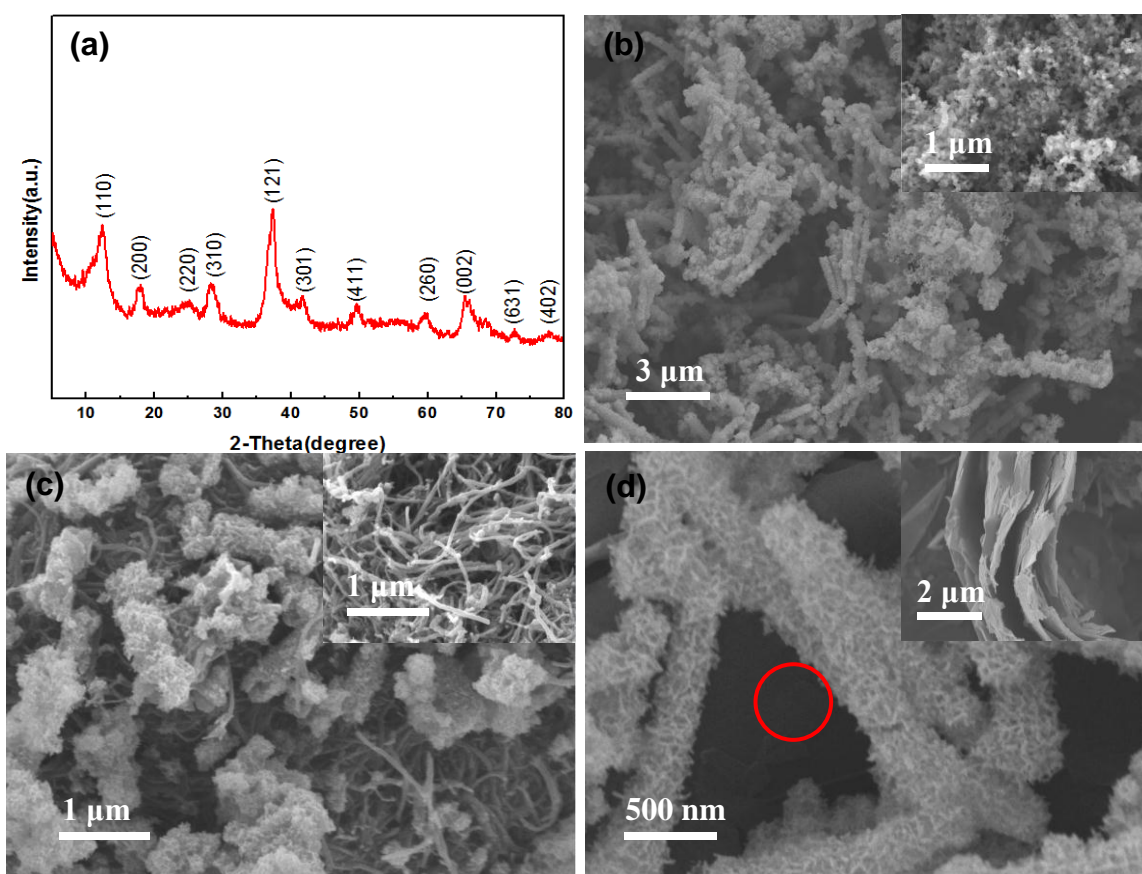


Figure 2. (a) XRD pattern of MnO₂ NTs and SEM images of MnO₂ nanotubes with graphene (b), carbon black (c), and carbon nanotubes (d), and the inner plot shows the SEM image of pure conductive additives.

Fig. 3 schematically illustrates the mixing process of the MnO_2 nanotubes with different conductive additives for working electrodes. The intimate mixtures were prepared by ultrasound, and MnO_2 nanotubes were blended with carbon black (0 D), carbon nanotubes (1 D), and graphene (2 D), all the conductive additives were well dispersed. However, the morphologies of various carbons materials have a significant impact on the charge transfer. Obviously, the carbon black particles connect each other with point contact, which certainly limits its conduction. What more, easy aggregation of carbon black particles lead to affect the charge-discharge rate. Carbon nanotubes as a fibrous additive cannot only form an effective conductive network, but also sustain the whole nanostructure with the binding force from the network. What's more, the graphene nanosheets have 2 D plate structures, but it seems unobvious in improving electrochemical properties due to the improper size. And the difference between three kinds of electrodes in electrochemical properties will be discussed in the next part.

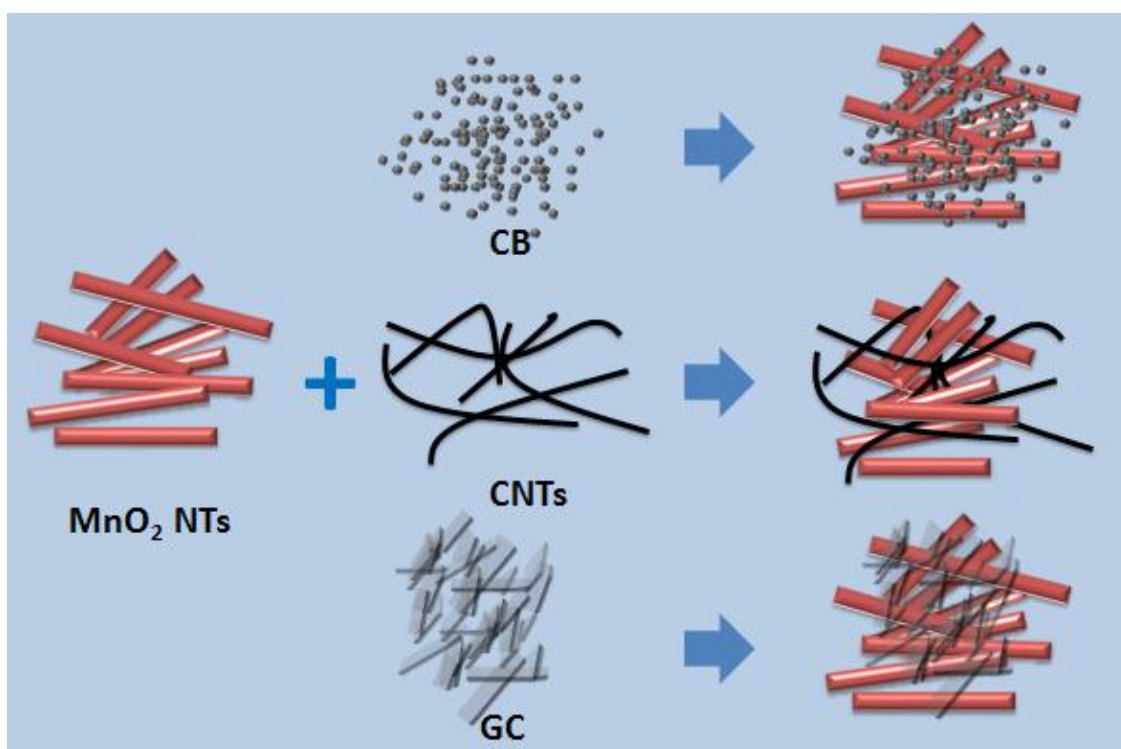


Figure 3. Schematic illustration shows the mixing process of MnO_2 nanostructure with different conductive additives.

3.2. Electrochemical performance of electrodes with different conductive additives

To identify the effective connect and charges transfer between MnO_2 nanotubes and conductive additives, the electrochemical performance of the MnO_2 nanotubes with different conductive agent electrodes were investigated. Herein, the three-electrode system using Pt foil as the counter electrode, and normal calomel electrode as the reference electrode. CV curves of different conductive additives at 50 mV s^{-1} are displayed in Fig.4a, the rectangular shape of the three curves were so similar, which

indicated that all the electrodes have excellent stability. This result was attributed to the large specific capacitance of MnO₂ nanotubes.

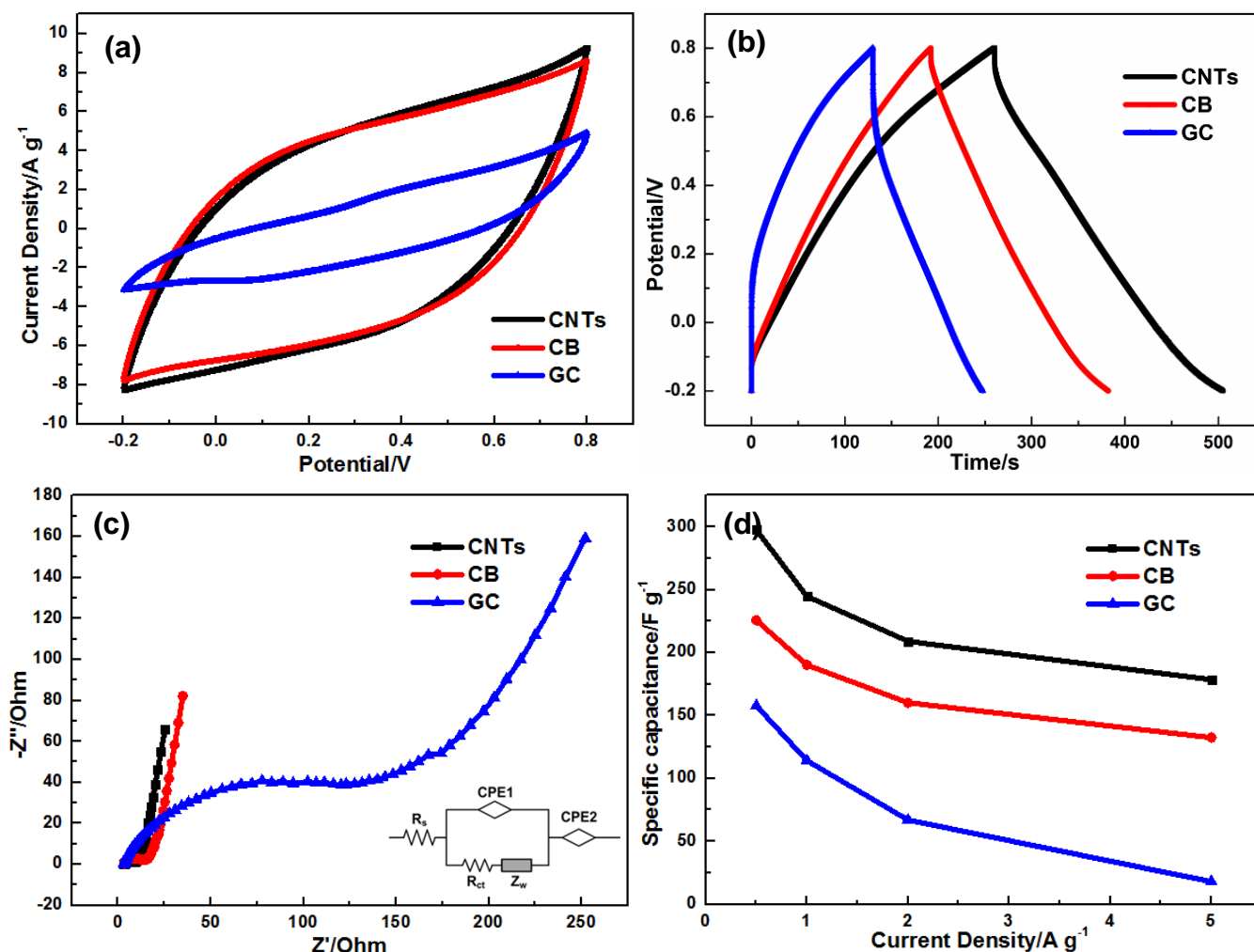


Figure 4. (a) Cyclic voltammograms of these electrodes at the scan rate of 50 mV s⁻¹ in a 1 M Na₂SO₄ aqueous electrolyte; (b) Charge-discharge curves of MnO₂ electrodes at current densities of 2 A g⁻¹; (c) The electrochemical impedance spectrum of the MnO₂ electrodes with different conducting additives in the frequency range from 0.01 Hz to 10 kHz and (d) Specific capacitance of MnO₂ nanostructures measured with different conducting additives.

However, the conductive additives impact the capacitance to a large extent. MnO₂@graphene electrode shows a distinct decrease in the capacitance, suggesting that graphene sheets had aggregated and impact its specific surface area and electrochemical properties. Based on the research by Jiang et al. indicated that the specific capacitor of pure graphene used in supercapacitors at 1 A g⁻¹ is 13 F g⁻¹ and the Na₂SO₄ electrolyte is not a suitable for graphene based materials to get high double-layer capacitances [34]. Graphene may be more suitable for negative electrode materials to reflect its excellent properties than that for conductive agent in positive electrode [35-36]. What's more, the cyclic voltammograms curves of MnO₂@carbon nanotubes electrode and MnO₂@carbon black particles electrode show a similar electrochemical properties in specific capacitance, which is better in

electrode needs further exploration. The sloped charge-discharge curves in potential window -0.2-0.8 V were investigated, as shown in Fig.4b, the electrode of MnO₂ nanotubes with carbon nanotubes shows significant advantages over other electrodes at the same current density. This result suggests that carbon nanotubes have higher value in improving charge storage capability, and we can image that these soft thin nanotubes can be intertwined with each other to form a powerful network to provide high conduction which was examined in SEM image (Fig. 2c). Additionally, it is obvious that there is a distinct potential drop (iR-drop) at the first few times of discharge process, which indicated that the carbon nanotubes owned the lowest resistance from the smallest iR-drop among the three kinds of conductive additives.

For comparison, the Nyquist plots of MnO₂ nanotubes with different additives have been included in Fig. 4c. Electrochemical impedance spectroscopy (EIS) spectra are often used to describe the electrochemical properties of supercapacitor, such as ion transfer and electrical conductivity. The semicircle at high-to-medium frequencies characterized the charge-transfer and the slope of the inclined line at low frequency represents the diffusion resistance. Or to be more precise, the starting point in the line at high frequency represent the sum impedance of the ionic resistance of electrolyte, electrodes, and the contact resistance between electrodes and current collector, which marked with R_s in the equivalent circuit. The diameter of the semicircles at the medium frequency indicates the interfacial charge transfer resistance, and R_{ct} used to express the resistance in the equivalent circuit. The slope of the line at the low-frequency refers to diffusivity resistance of the electrolyte and marked with Z_w (Warburg impedance) [8]. It is obvious that the MnO₂@carbon nanotubes electrodes showed a much smaller charge transfer resistance (R_{ct}) compared to other electrodes, and the internal resistances of three different electrodes extremely close, which suggest that the conductivities of three conductive additives are all excellent. While, the lower charge-transfer resistance of MnO₂@carbon nanotubes electrode as measured the semicircle at high-to-medium frequencies may due to that carbon nanotubes has a one-dimensional multiaperture structure which comes into a fibrous network and builds an expressway for charge-transfer to improve the electrical conductivity and chemical stability. And from the numerical simulation by Dalmas also demonstrate the comparison of percolation threshold between carbon nanotubes and carbon black particles [37]. The electronic conductivity of three kinds of these conductive agents are in turn carbon nanotubes > carbon black particles > graphene, which is conforms with the above analysis.

What's more, the specific capacitance of the electrodes can be calculated from the GCV curves using the following equation:

$$C_m = I t / \Delta V m \quad (1)$$

Where C_m denote the specific capacitance ($F g^{-1}$), t is the discharge time (s), m is the weight of active materials (g), I and ΔV are the current density (A) and potential range (V) during the process of charge-discharge. The specific capacitance of MnO₂@carbon nanotubes electrode reaches $244.8 F g^{-1}$ at current density of $1 A g^{-1}$, and the specific capacitances of electrodes MnO₂@carbon black particles and MnO₂@graphene are $190.2 F g^{-1}$ and $114.1 F g^{-1}$ respectively. In addition, the specific capacitance of MnO₂@ carbon nanotubes electrode still remains its highest quality reach at $178.5 F g^{-1}$ even when the current density is increased to $5 A g^{-1}$, and the MnO₂@carbon black particles electrode

decrease to 132.5 F g^{-1} , MnO_2 @graphene, 18 F g^{-1} respectively. Taken together, MnO_2 @carbon nanotubes electrode is optimal in these electrodes.

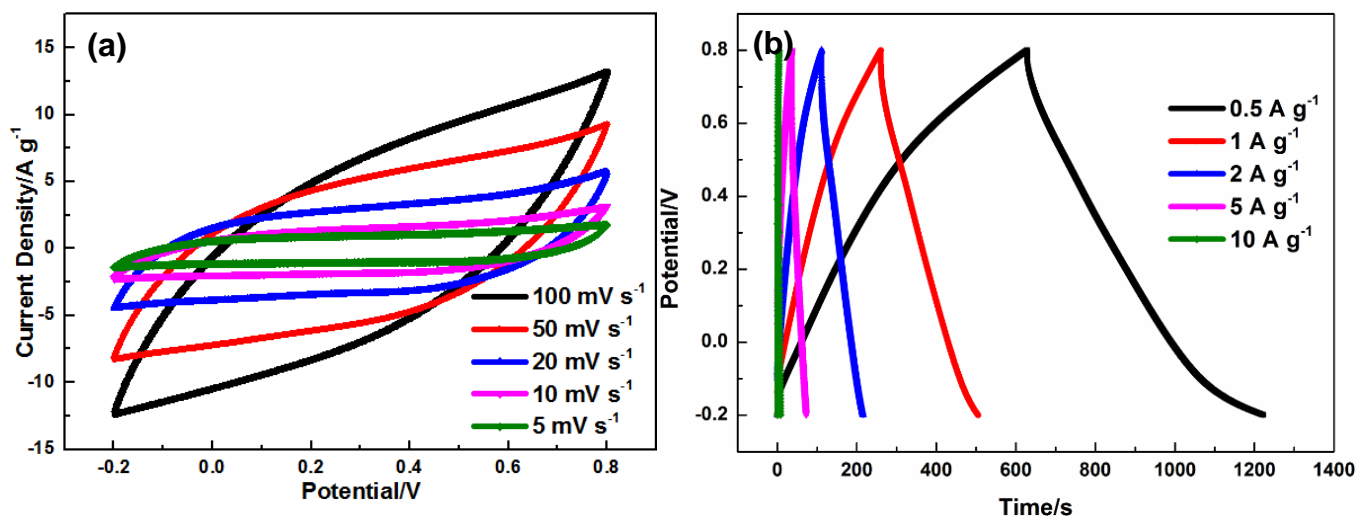


Figure 5. (a) Cyclic voltammograms of MnO_2 @carbon nanotubes electrodes at different scan rate (5, 10, 20 50 and 100 mV s^{-1}) in a $1 \text{ M Na}_2\text{SO}_4$ aqueous electrolyte; (b) Charge-discharge curves at different current densities ($0.5, 1, 2, 5$ and 10 A g^{-1}).

Concretely, the curve of MnO_2 nanotubes with carbon nanotubes shows a relatively good capacitive behavior as the conductive agent. And the electrochemical performance of the MnO_2 @carbon nanotubes electrode is investigated in a three-electrode configuration. Fig.5a shows the CV curves of MnO_2 @ carbon nanotubes electrode at various scan rates from 5 to 100 mV s^{-1} with a voltage window of -0.2 V - 0.8 V . The shape of the curves outline show no significant redox peaks suggests ideal capacitive behavior of MnO_2 @carbon nanotubes electrode. Moreover, the current response would gradually increase with the increased scan rates, which caused by the reason that there is no enough time at high scan rate to make ions transfer around the circuit. But all the curves are very similar and show a quasi-rectangular shape as the scan rate increases to 100 mV s^{-1} , revealing the electrode had an ideal pseudocapacitive behavior with a much enhanced high rate capability and its favorable charge and discharge characteristic is further supported by the symmetric triangular shape of galvanostatic charge/discharge profiles as show in Fig.5b. It is well known that the ohmic polarization is linear with current, which not only impact the capacitance but also decreases the discharge time as current increases. The good symmetry of the GCD curves validates its efficient capacitive behavior, which indicated that the carbon nanotubes had substantially improved the capacitance and charge-discharge rate of MnO_2 nanotubes under all the current densities. Anyway, the combination of the MnO_2 nanotubes and carbon nanotubes not only increased conductivity and electrolyte accessibility, but also provided high surface area and excellent mechanical properties. Currently, the industrial production is quite qualified for the mass production of carbon nanotubes and guarantees the performance. In all fairness, the carbon nanotubes can be a better choice as high-power applications at around the same price when compared with other conductive additives.

4. CONCLUSIONS

In summary, we have demonstrated a comparison between different conductive additives to impact the electrochemical properties of MnO₂ nanotubes. The electrochemical performances of these electrodes were investigated by a three-electrode system, and the working electrodes were prepared by a simple physical procedure of MnO₂ nanotubes, conductive additives and NMP with the proportion of 7:2:1. The nanocomposites electrodes in our work all revealed excellent pseudocapacitance performance due to the electrochemical properties of MnO₂ nanotubes. Furthermore, the specific conductivity of MnO₂@carbon black electrode, MnO₂@carbon nanotubes, MnO₂@graphene electrodes at the current density 1 A g⁻¹ is 244.8 F g⁻¹, 190.2 F g⁻¹, and 114.1 F g⁻¹ respectively. The MnO₂@ carbon nanotubes electrode showed not only improves the electrical conductivity of the MnO₂@carbon black particles and MnO₂@graphene electrode, but also extends the discharge time. The maximum specific capacitance for MnO₂@carbon nanotubes electrode reaches 297.5 F g⁻¹ at the current density 0.5 A g⁻¹ and still remains at 178.5 F g⁻¹ (60% retention) even when the current density increased to 5 A g⁻¹, which can be put down to these soft thin nanotubes can be intertwined with each other to form a powerful network to provide conduction. The high specific capacitance and excellent charge-discharge rate of the MnO₂@carbon nanotubes electrode ensures its potential for the applications in supercapacitors and other microelectronics.

ACKNOWLEDGEMENT

The authors gratefully acknowledge the financial supports provided by State Education Ministry and Fundamental Research Funds for the Central Universities (Chongqing University).

References

1. Z.M. Hu, X. Xiao, C. Chen, T.Q. Li, L. Huang, C.F. Zhang, J. Su, L. Miao, J.J. Jiang, Y.R. Zhang, J. Zhou, *Nano Energy*, 11 (2015)226.
2. X.S. Hu, L. Johannesson, N. Murgovski, B. Egardt, *Applied Energy*, 137 (2015) 913.
3. Y.F. Tang, T. Chen, S.X. Yu, Y.Q. Qiao, S.C. Mu, S.H. Zhang, Y.F. Zhao, L. Hou, W.W. Huang, F. Gao, *Journal of Power Sources*, 295 (2015) 314.
4. H.L. Li, L.X. Jiang, Q.L. Cheng, Y. He, V. Pavlinek, P. Saha, C.Z. Li, *Electrochimica Acta*, 164 (2015) 252.
5. Y. Tian, Z.Y. Liu, R. Xue, L.P. Huang, *Journal of Alloys and Compounds*, 671 (2016) 312.
6. M. Huang, F. Li, F. Dong, Y.X. Zhang, L.L. Zhang, *J. Mater. Chem. A*, 3 (2015) 21380.
7. M. Huang, F. Li, X.L. Zhao, D. Luo, X.Q. You, Y.X. Zhang, G. Li, *Electrochimica Acta*, 152 (2015) 172.
8. M. Lee, S.K. Balasingam, H.Y. Jeong, W.G. Hong, H.B.R. Lee, B.H. Kim, Y. Jun, *Scientific Reports*, 5 (2015) 8151.
9. B.G.S. Raj, A.M. Asiri, J.J. Wu, S. Anandan, *Journal of Alloys and Compounds*, 636 (2015) 234.
10. S. Chen, C.H. Wu, A. Fang, C.K. Lin, *Ceramics International*, 42 (2016) 4797.
11. J.H. Kim, K.H. Lee, L.J. Overzet, G.S. Lee, *Nano Lett.* 11 (2011) 2611.
12. X.H. Su, L. Yu, G. Cheng, H.H. Zhang, M. Sun, X.F. Zhang, *Applied Energy*, 153 (2015) 94.
13. K.W. Qiu, Y. Lu, D.Y. Zhang, J.B. Cheng, H.L. Yan, J.Y. Xu, X.M. Liu, J.K. Kim, Y.S. Luo, *Nano Energy*, 11 (2015) 687.
14. S.J. He, W. Chen, *Journal of Power Sources*, 294 (2015) 150.

15. X.L. Guo, G. Li, M. Kuang, L. Yu, Y.X. Zhang, *Electrochimica Acta*, 174 (2015) 87.
16. R.T. Vinny, K. Chaitra, K. Venkatesh, N. Nagaraju, N. Kathyayini, *Journal of Power Sources*, 309 (2016) 212.
17. F. Li, Y.X. Zhang, M. Huang, Y. Xing, L.L. Zhang, *Electrochimica Acta*, 154 (2015) 329.
18. Z.N. Yu, L. Tetard, L. Zhai, J. Thomas, *Energy Environ. Sci.*, 8 (2015) 702.
19. Y. Wang, P.S. Ding, C. Wang, *Journal of Alloys and Compounds*, 654 (2016) 273.
20. H. Chen, B. Zhang, F. Li, M. Kuang, M. Huang, Y. Yang, Y.X. Zhang, *Electrochimica Acta*, 187 (2016) 488.
21. A. Zolfaghari, H.R. Naderi, H.R. Mortaheb, *Journal of Electroanalytical Chemistry*, 697 (2013) 60.
22. X.L. Wang, X.Y. Fan, G. Li, M. Li, X.C. Xiao, A.P. Yu, Z.W. Chen, *Carbon*, 93 (2015) 258.
23. S. Chen, J.W. Zhu, X. Wang, *ACS nano*, 10 (2010) 6212.
24. Y.Y. Shang, Z. Yu, C. Xie, Q.X. Xie, S.H. Wu, Y.F. Zhang, Y.F. Guan, *J Solid State Electrochem*, 19 (2015) 949.
25. L.L. Zhang, X. S. Zhao, *Chem. Soc. Rev.*, 38 (2009) 2520.
26. S.L. Kuo, N.L. Wu, *Journal of Power Sources*, 162 (2006) 1437.
27. Y.X. Zhang, M. Kuang, M. Huang, Z.Q. Wen, *Int. J. Electrochem. Sci.*, 8 (2013) 9723.
28. M. Inagaki, H. Konno and O. Tanaike, *J. Power Sources*, 195 (2010) 7880.
29. Y.W. Zhu, S. Murali, M.D. Stoller, K. J. Ganesh, W.W. Cai, P. J. Ferreira, A. Pirkle, R.M. Wallace, K.A. Cychosz, M. Thommes, D. Su, E.A. Stach, R.S. Ruoff, *Science*, 332 (2011) 1537
30. S. Nardecchia, D. Carriazo, M.L. Ferrer, M.C. Gutierrez, F.D. Monte, *Chem. Soc. Rev.*, 42 (2013) 794.
31. X.Y. Cai, S.H. Lim, C.K. Poh, L.F. Lai, J.Y. Lin, Z.X. Shen, *Journal of Power Sources*, 275 (2015) 298.
32. Y.X. Zhang, M. Huang, F. Li, Z.Q. Wen, *Int. J. Electrochem. Sci.*, 8 (2013) 8645.
33. M. Huang, Y.X. Zhang, F. Li, Z.C. Wang, Alamusi, N. Hu, Z.Y. Wen, Q. Liu, *Scientific Reports*, 4 (2014) 4518.
34. R.Y. Jiang, C.Y. Cui, H.Y. Ma, *Electrochimica Acta*, 104 (2013) 198.
35. X.M. Mu, X.Z. Liu, K. Zhang, J. Li, J.Y. Zhou, E.Q. Xie, and Z.X. Zhang, *Electron. Mater. Lett.*, Vol. , 2 (2016) 296.
36. X. Yang, F.Y. Qu, H. Niu, Q. Wang, J. Yan, Z.J. Fan, *Electrochimica Acta*, 180 (2015) 287.
37. F. Dalmás, R. Dendievel, L. Chazeau, J. Cavaillé, C. Gauthier, *Acta Mater.*, 54 (2006) 2923.